WILEY

Multiscale and macroscopic modeling of magneto-elastic behavior of soft magnetic steel sheets

Dries Vanoost[1] [ID] | Simon Steentjes[2] | Joan Peuteman[1] | Herbert De Gersem[3, 4] |
Davy Pissoort[1] | Kay Hameyer[2]

[1]Research Group ReMI, KU Leuven Technology Campus Ostend, B-8400, Ostend, Belgium

[2]Institute of Electrical Machines, RWTH Aachen University, Aachen, D-52062, Germany

[3]Department of Physics and Astronomy, Solid-State Physics and Magnetism, Ku Leuven, Leuven, Belgium

[4]Institut fur Theorie Elektromagnetischer Felder, TU Darmstadt, Darmstadt, D-64283, Germany

Correspondence
Dries Vanoost, Research Group ReMI, KU Leuven Technology Campus Ostend, B8400 Ostend, Belgium.
Email: dries.vanoost@kuleuven.be

Abstract

This paper compares different energy-based magneto-mechanical models, which describe the magnetization changes that a magnetostrictive and anisotropic material undergoes when subjected to a quasi-static H-field excitation and tensile or compressive external stress. The magnetic behavior is either characterized by considering the phenomenological energy-based Hauser hysteresis model or by the recently introduced hysteresis energy. The effect of mechanical stress is included naturally in the energy summation of the multiscale models. Properties of the different models, such as accuracy and parameter identification, are illustrated by comparison with experimental data for a nonoriented FeSi3% electrical steel grade.

KEYWORDS
hysteresis loops, magneto-mechanical couplings, magnetostatics, micromagnetics, multiscale modeling, nonlinear magnetics

1 | INTRODUCTION

When designers optimize their design of an actuator, they mainly focus on the geometry of the design without the support of the material and/or the material models. As shown in Bernard at al and Ganet et al,[1,2] the operation mode of the actuator generates additional mechanical stress, which alters the material behavior. This is known as the inverse magnetostrictive effect (Villari effect), which was found in 1865.[3] Villari realized the correlation between a magnetization change and the tensile stress of iron-based materials. In general, the mechanical stress does not only affect the permeability of the material, but it also affects the area and the shape of the hysteresis loop,[4-8] mainly described with the coercivity and remanence of the hysteresis loop.

To include the influence of mechanical stress in the design process, electrical engineers require highly accurate models for the soft magnetic material behavior. These should be able to properly represent the hysteresis and magnetostriction effect of different materials without the need of tedious parameter identifications. Tedious parameter identifications as required by the phenomenological macroscopic models like the Jiles-Atherton-Sablik model[9] or the Preisach model[10] rest on a huge amount of measured data. Therefore, these models give a mathematical representation of the measured data with low predictive capabilities. This is a strong point because the conditions that prevail in real-life application are much more diverse than standardized experimental conditions. In addition, the multiaxiality and material heterogeneity have to be included.

An option to include these phenomenons is to resort to micromagnetic models, which make predictions of the magnetic behavior based on the micromagnetic domain theory. Because they use the domain and/or grain scale, they are able to use the energy density function as an investigation tool to predict the magnetic behavior of a crystal.[11-13] The obtained

minimum of the energy density function describes the magnetic state of the domain, which depends on the externally applied stress and the magnetic field as well as the eigen stress[14,15] and the magnetic field. The major disadvantage of these micromagnetic models is the computational cost. Because of this reason, these models are not appropriate for 3D or 2D simulations of macroscopic applications.

To make affordable simulations, without loosing the physical origins, multiscale models deliver a solution. These models use the same energy density function as an investigation tool to predict the magnetic behavior of a crystal. By applying various spatial scales with appropriate homogenization procedures, they allow one to simulate the same complexity of the magneto-elastic coupling of a polycrystalline material with a reduced cost. This paper focuses on models that are based on the multiscale energy-based material model by Daniel et al.[16] This material model originally was anhysteretic. In this paper, we focus on 3 variants, which include the hysteresis effect in the model. Two models originate from the same research group and the last model is our own variation on this multiscale model.[17]

The paper is organized as follows. In Section 2, the energy density function of a cubic crystal is recapitulated, as well as the new energy function[17] to include hysteresis effect. Section 3 describes the 2 homogenization procedures, from the crystal scale to the grain scale and from the grain scale to the polycrystalline scale. Section 5 describes the differences between the material models and compares the results of the material models for FeSi3%. Section 6 summarizes the paper and formulates conclusions.

2 | DOMAIN SCALE

At the domain scale, the energy density function describing the ferromagnetic behavior of a single crystal is valid. As described in the previous studies,[16-20] some assumptions are made. As an example, a uniform strain and a uniform magnetic field are considered at this scale so the exchange energy can be neglected. The domain scale is the smallest scale leading to the "constitutive law." Depending on the used material model, the anhysteretic approach for the magneto-elastic coupling[6,21] is used, or as in our previous work,[17,22,23] the hysteresis effect is also introduced at this scale. First, the anhysteretic description of the reversible magneto-elastic behavior is recapitulated. Finally, the hysteresis energy density function, introduced in the previous studies,[17,22,23] is briefly recalled.

2.1 | Anhysteretic approach for magneto-elastic coupling

This work is derived from the reversible magneto-elastic behavior,[16] which is based on the definition of the free energy of the material at the domain scale. The free energy density function W_α consists of 3 terms for the anhysteretic approach, namely, (1) the Zeeman energy density function W_H (Equation 1), (2) the magneto-crystalline anisotropy energy density W_{an} (Equation 2), and (3) the stress induced anisotropy energy density W_σ (Equation 3).

The Zeeman energy density function W_H (Equation 1) describes the effect of the magnetic field $H = [H_1, H_2, H_3]$ on the magnetic domains this by calculating the amount of energy required to rotate the magnetization $M_s[\alpha_{M1}, \alpha_{M2}, \alpha_{M3}]$ away from the direction of the magnetic field.[19,24] Here, M_s is the saturation magnetization of the material and $[\alpha_{M1}, \alpha_{M2}, \alpha_{M3}]$ are the cosine directions of the possible magnetization states. μ_0 is the permeability of vacuum.

$$W_H = -\mu_0 M_s \left(\alpha_{M1} H_1 + \alpha_{M2} H2 + \alpha_{M3} H_3 \right). \quad (1)$$

The magneto-crystalline anisotropy energy density W_{an} (Equation 2) describes the effect of the easy directions of the crystal on the magnetic domains. Depending on the crystal type, some directions are more preferred than others and they are called the easy directions. The least preferred directions are called the hard directions.[19,24] The magneto-crystalline anisotropy energy density W_{an} (Equation 2) describes the amount of energy required to rotate the magnetization $M_s[\alpha_{M1}, \alpha_{M2}, \alpha_{M3}]$ away from an easy direction to a less preferred direction.[19,24] For a cubic crystal, the magneto-crystalline anisotropy energy density function W_{an} is obtained using the crystal anisotropic constants K_1 and K_2.

$$\begin{aligned} W_{an} = &K_1[(\alpha_{M1})^2(\alpha_{M2})^2 + (\alpha_{M2})^2(\alpha_{M3})^2 + (\alpha_{M3})^2(\alpha_{M1})^2] \\ &+ K_2[(\alpha_{M1})^2(\alpha_{M2})^2(\alpha_{M3})^2] \end{aligned}$$

$$(2)$$

The stress-induced anisotropy energy density function W_σ (Equation 3) describes the effect of a mechanical stress on the magnetic easy direction of the crystal. When applying a mechanical stress to a crystal structure, it starts to deform. This deformation affects the easy and the hard directions of the crystal, that is, some directions become more preferred while others become less preferred compared to the situation without mechanical stress. In other words, a correction on the magneto-crystalline anisotropy energy density function W_{an} is required when a stress is applied. For a cubic crystal, the stress-induced anisotropy energy density function W_σ is obtained using the saturation magnetostrictions λ_{100} and λ_{111}, (respectively in the 100 direction and the 111 direction) and the stress. Equation 3 uses the Mandel notation,[25] vectorizing the stress as $\sigma = [\sigma_{11}, \sigma_{22}, \sigma_{33}, \sigma_{23}, \sigma_{13}, \sigma_{12}]$.

$$W_\sigma = -\frac{3}{2}\lambda_{100}\left[\sigma_{11}\left((\alpha_{M1})^2 - \frac{1}{3}\right) + \sigma_{22}\left((\alpha_{M2})^2 - \frac{1}{3}\right) + \sigma_{33}\left((\alpha_{M3})^2 - \frac{1}{3}\right)\right]$$
$$- 3\lambda_{111}\left[\sigma_{23}(\alpha_{M2}\alpha_{M3}) + \sigma_{13}(\alpha_{M1}\alpha_{M3}) + \sigma_{12}(\alpha_{M1}\alpha_{M2})\right]$$

(3)

This equation is only valid when the magnetostrictive strain (Equation 4) is isochore,[16] implying that the magnetostrictive strain is described using only the saturation magnetostrictions λ_{100} and λ_{111}. When the crystal structure is perfect, the magnetization will align with the cosine direction $\gamma = [\gamma_1, \gamma_2, \gamma_3]$, which is the direction with the lowest total internal energy density ($W_\alpha(\gamma) = \min(W_\alpha)$) with W_α consisting of the sum of the 3 energy densities (Equation 5). W_α depends on the cosine directions of the possible magnetization states. The free energy density function W_α leads to the probability function of the anhysteretic part for magneto-elastic coupling, see Section 3.1.

$$\varepsilon_\mu = \frac{3}{2}\begin{bmatrix} \lambda_{100}\left(\gamma_1^2 - 1/3\right) \\ \lambda_{100}\left(\gamma_2^2 - 1/3\right) \\ \lambda_{100}\left(\gamma_3^2 - 1/3\right) \\ \lambda_{111}\sqrt{2}\gamma_2\gamma_3 \\ \lambda_{111}\sqrt{2}\gamma_1\gamma_3 \\ \lambda_{111}\sqrt{2}\gamma_1\gamma_2 \end{bmatrix}.$$

(4)

$$W_\alpha = W_H + W_{an} + W_\sigma.$$

(5)

2.2 | Hysteretic approach for magneto-elastic coupling

As described in the previous studies,[17,22,23] the work describing the reversible magneto-elastic behavior[16] does not account for the magnetization state at an earlier time step. By introducing an additional energy density function to the free energy density function, at the domain scale, the irreversible effect is added. The hysteresis energy density function (Equation 6) describes the effect of the previous magnetization state on the new magnetization state. This can be explained using the energy landscape,[17] which visualizes how a magnetic domain can be trapped in a local minimum in the energy landscape.

The hysteresis energy density function uses the demagnetization field, which is obtained by the magnetization of the previous step $M_{hys} = [M_{hys1}, M_{hys2}, M_{hys3}]$ and divided by the magnetic susceptibility χ_0. This equation resembles the Zeeman energy density function (Equation 1). The hysteresis energy density function will lead to the additional probability function of the hysteretic part for magneto-elastic coupling.

$$W_{hys} = -\mu_0\frac{M_s}{\chi_0}\left(\alpha_{M1}M_{hys1} + \alpha_{M2}M_{hys2} + \alpha_{M3}M_{hys3}\right) \quad (6)$$

3 | HOMOGENIZATION

In the full multiscale energy-based material model, 2 homogenization processes are required. The first homogenization process relates the domain scale to the grain scale and is called the "constitutive law". Depending on the used material model, this constitutive law can either be anhysteretic[6,21] or hysteretic.[17,22,23] The second homogenization process maps the grain scale to the polycrystalline scale, which makes use of the properties, interactions, and orientations of the individual grains to obtain the effective elastic and magnetic properties of the polycrystalline material. This homogenization is obtained using a self-consistent polycrystalline scheme, based on the work of Hill,[15] Kröner,[15] and Eshelby,[14] better known as the Eshelby inclusion problem.

3.1 | Constitutive law

The constitutive law starts from the free energy density function W_α (Equation 5) of a domain. W_α leads to the volume fraction of the magnetic moments in a grain, by implying it in an explicit Boltzmann-type relation. This distribution leads to the grain magnetization M_g and the grain magnetostriction ε_g. The distribution is obtained using a Boltzmann distribution with an adjustable material parameter A_s for the anhysteretic constitutive law (Equation 7). The material parameter A_s accounts for the domain walls, the nonuniformity of the mechanical stress and/or magnetic fields, and other crystal defects.

$$P_\alpha = \frac{\exp(-A_s(W_H + W_{an} + W_\sigma))}{\int_\alpha \exp(-A_s(W_H + W_{an} + W_\sigma))} \quad (7)$$

$$P_{hys} = \frac{\exp(-\beta A_s W_{hys})}{\int_\alpha \exp(-\beta A_s W_{hys})} \quad (8)$$

$$P_g = \frac{P_\alpha P_{hys}}{\int_\alpha P_\alpha P_{hys}} \quad (9)$$

The probability obtained with Equation 7 is derived in Daniel et al[16] and describes the anhysteretic distribution function. To introduce the irreversible work, an additional Boltzmann distribution function using the hysteresis energy density function

was suggested in the previous studies[17,22,23] with an additional material parameter β for the hysteretic constitutive law (Equation 8). The material parameter β accounts for defocus of the local magnetization because of crystal defects as well as the rotation mechanism and the pinning effect.[19] As suggested by Hauser,[26] the irreversible work due to pinning affects the probability density.

$$M_g = \begin{bmatrix} \int_\alpha P\, \alpha_{M1}\, M_s \\ \int_\alpha P\, \alpha_{M2} M_s \\ \int_\alpha P\, \alpha_{M3} M_s \end{bmatrix} \tag{10}$$

$$\varepsilon_g = \begin{bmatrix} \int_\alpha P\, \frac{3}{2}\lambda_{100}\left(\alpha_{M1}^2 - \frac{1}{3}\right) \\ \int_\alpha P\, \frac{3}{2}\lambda_{100}\left(\alpha_{M2}^2 - \frac{1}{3}\right) \\ \int_\alpha P\, \frac{3}{2}\lambda_{100}\left(\alpha_{M3}^2 - \frac{1}{3}\right) \\ \int_\alpha P\, \frac{3}{2}\lambda_{111}\left(\sqrt{2}\alpha_{M2}\alpha_{M3}\right) \\ \int_\alpha P\, \frac{3}{2}\lambda_{111}\left(\sqrt{2}\alpha_{M1}\alpha_{M3}\right) \\ \int_\alpha P\, \frac{3}{2}\lambda_{111}\left(\sqrt{2}\alpha_{M1}\alpha_{M2}\right) \end{bmatrix} \tag{11}$$

Then the probability function of the grain (Equation 9) is the normalization of Equations 7 and 8 as shown in Equation 9. Depending on using the anhysteretic or hysteretic constitutive law, the grain magnetization and magnetostriction are obtained by using Equations 7 and 9 respectively for P in Equations 10 and 11.

3.2 | Eshelby inclusion problem

To take into account the properties, interactions, and orientations of the individual grains, to obtain the effective elastic and magnetic properties of the polycrystalline material, a self-consistent polycrystalline scheme is used. This self-consistent polycrystalline scheme, known as Eshelby inclusion problem, is described in the previous studies.[6,14-17] This self-consistent polycrystalline scheme converts the externally applied stress σ_m and the magnetic field $\vec{H}_m$ to the locally applied stress σ_g and the magnetic field $\vec{H}_g$ using localization Equations 12 and 13. These localization equations do not only convert the σ_m and $\vec{H}_m$ to the crystallographic orientation frame of the considered grain but also include the influence of the medium surrounding the considered grain. Applied on the stress (Equation 12), the local stress σ_g consists of the external mechanical stress and the residual mechanical stress. The first term is a purely elastic problem, which assumes that the considered grain is an inclusion in a homogeneous material that is solved using the stress-concentration B_g. The second term exists because of the eigenstrain, in this case, the magnetostriction and the stiffness of the surrounding medium, which is solved using the elastic

incompatibility tensor L_g^σ. B_g as well as L_g^σ only depend on the elastic stiffness coefficients C_{ij} of a single crystal.

$$\sigma_g = B_g^\sigma : \sigma_{ext} + L_g^\sigma : \left(\epsilon_m^\mu - \epsilon_g^\mu\right) \tag{12}$$

Applied on the magnetic field (Equation 13), the local magnetic $\vec{H}_g$ consists of the externally applied magnetic field $\vec{H}_m$ and the demagnetizing field. The first term is the externally applied magnetic field $\vec{H}_m$ transformed to the crystal reference frame. The second term is the demagnetizing field, originating from the difference between the macroscopic magnetization $\vec{M}_m$ and the grain magnetization $\vec{M}_g$ divided by the equivalent media susceptibility.[16]

$$\vec{H}_g = \vec{H}_m + \frac{1}{3 + 2\chi_m}\left(\vec{M}_m - \vec{M}_g\right) \tag{13}$$

When using the demagnetizing field in the constitutive law, by using the hysteresis energy density function, Equation 13 is not used and $\vec{H}_m$ is only rotated to the crystal reference frame. The locally obtained mechanical stress σ_g and $\vec{H}_g$ obtained for every grain lead to the local mechanical strain ε_g and $\vec{M}_g$ by using the constitutive law, see Section 3.1. When $\vec{M}_g$ and ε_g are obtained for every grain, the macroscopic magnetization $\vec{M}_m$ and the magnetostriction ε_m are obtained with a weighted average based on the grain size:

$$\vec{M}_m = \left\langle \vec{M}_g \right\rangle \tag{14}$$

$$\varepsilon_m = \left\langle \varepsilon_m \right\rangle. \tag{15}$$

This self-consistent model requires an initial guess of $\vec{M}_m$ and ε_m to obtain the new solution of $\vec{M}_m$ and ε_m. By iteratively replacing the initial values with the new solutions, the self-consistent model converges.

4 | HAUSER HYSTERESIS MODEL AND STRESS-DEMAGNETIZATION EFFECT

In the material models where the hysteresis effect is not included in the constitutive law,[6,21] the irreversible work is included after the homogenization process, based on the work of Hauser.[26] The irreversible contribution $\vec{H}_g^{irr}$ (Equation 16) modifies the anhysteretic magnetic field $\vec{H}_g$ and is parallel to $\vec{H}_g$.

$$\left\|\vec{H}_g^{irr}\right\| = \delta\left(\frac{k_r}{\mu_0 M_s} + c_r\left\|\vec{H}_g\right\|\right)\left[1 - \kappa_g \exp\left(-\frac{k_a}{\kappa_g}\left\|\vec{M}_g - \vec{M}_g^{reb}\right\|\right)\right] \tag{16}$$

In this equation, δ equals ± 1, it start as $+1$ and every time the loading direction inverses the sign changes. The parameters k_r, c_r, k_a, and κ_g are material parameters, where κ_g also changes every time the loading direction is inverse (Equation 17). Here, κ_g^0 is the previous value of κ_g, and $\vec{M}_g^{reb}$ is the previous value of $\vec{M}_g$ when the loading direction is inverse.

$$\kappa_g = 2 - \kappa_g^0 \exp\left(-\frac{k_a}{\kappa_g^0}\left\|\vec{M}_g - \vec{M}_g^{reb}\right\|\right) \tag{17}$$

$$k_r = k_r^0\left(\frac{4}{3} - N_g\right) \tag{18}$$

The parameter k_r is determined by Equation 18, where k_r^0 is a material constant, which accounts for the stress effect on the coercive field. N_g (Equation 20) defines the "stress-demagnetization effect," which is also used to calculate the fictitious configuration field $\vec{H}_g^{conf}$ (Equation 19) to correct the model for changes in the domain configuration due to the applied stress. Here, η is a material parameter and σ_g^{eq} (Equation 21) is the equivalent stress for σ_g in the direction of the magnetic field ($\vec{h} = \vec{H}/\|\vec{H}\|$). The local effective field $\vec{H}_m^x$ (Equation 22) consists of the sum of the 3 field components $\vec{H}_g, \vec{H}_g^{conf}$, and $\vec{H}_g^{irr}$, which leads to the macroscopic effective field $\vec{H}_m^x$.

$$\vec{H}_g^{conf} = \eta\left(N_g - \frac{1}{3}\right)\vec{M}_g \tag{19}$$

$$N_g = \frac{1}{1 + 2\exp\left(-K\sigma_g^{eq}\right)} \tag{20}$$

$$\sigma_g^{eq} = \frac{3}{2}\vec{h}\left(\sigma_g - \frac{1}{3}tr\left(\sigma_g\right)I\right)\vec{h} \tag{21}$$

$$\vec{H}_m^x = \left\langle\vec{H}_g^x\right\rangle = \left\langle\vec{H}_g + \vec{H}_g^{conf} + \vec{H}_g^{irr}\right\rangle \tag{22}$$

5 | COMPARING MODELS

In this section, 3 energy-based models are compared with each other and with a number of measurements. The energy-based material model uses the theory described in Sections 2 to 2.2. The models are the simplified model of Daniel et al,[21] the full multiscale energy-based material model of Daniel et al,[6] and the own model introduced in Vanoost et al.[17] The measurement results are obtained from Rekik.[27]

5.1 | Measurements

The models are compared based on a positive magnetostrictive material FeSi3%, which suffers from the nonmonotonic effect.[6,17,21,27] The measurement results are shown in Figure 3.

5.2 | Simplified material model of Daniel et al

Figure 1 shows the simplified model of Daniel et al.[21] The simplification consists of considering the material as a single crystal, where the energy density functions are converted to address the macroscopic behavior instead of the micromagnetic behavior using Equations 23, 25, and 26. The main modification occurs to the anisotropic energy density function (Equation 26), which is an uniaxial anisotropy along the β direction. The energy functions are used in the Boltzmann distribution, as described in Section 3.1, to obtain the anhysteretic distribution P_α (Equation 7). The parameters used to obtain the simulation results of Figure 3 are given in Table 1. The material parameters are obtained by measurements.[21] The anhysteretic parameters, M_s and λ_s, are the maximum obtained magnetization and magnetostriction of the material when no stress is applied. Based on an anhysteretic measurement, A_s is obtained. η requires a susceptibility measurement under stress. The 4 parameters describing the hysteresis effect are obtained according to Hauser.[26] They require a major hysteresis loop when no stress is applied.

$$W_H = -\mu_0\vec{H}\vec{M}_\alpha \tag{23}$$

$$\varepsilon = \lambda_s\left(\frac{3}{2}\vec{\alpha}_m\vec{\alpha}_m^T - \frac{1}{2}I\right) \tag{24}$$

$$W_{sigma} = -\sigma : \varepsilon \tag{25}$$

$$W_{an} = -J(\alpha\beta)^2 \tag{26}$$

5.3 | Full material model of Daniel et al

Figure 2 shows the full model of Daniel et al.[6] The main difference between the simplified model and the full model is the use of the self-consistent polycrystalline scheme as described in Section 3.2, which requires crystallographic texture data of the material and the anhysteretic constitutive law. The energy function at the constitutive law is used in the Boltzmann distribution, as described in Section 3.1 to obtain the anhysteretic distribution P_α (Equation 7). The parameters used to obtain the simulated results of Figure 3 are given in Table 2. As described in Daniel et al,[6] the material parameters are identified using anhysteretic measurements at low fields
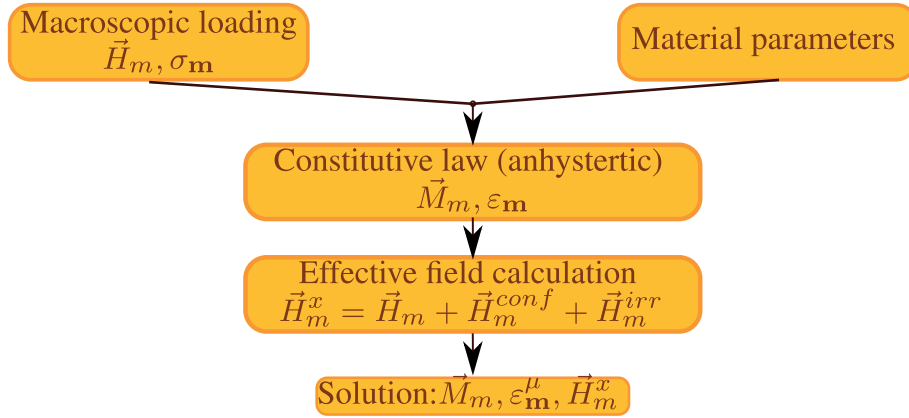
FIGURE 1 Flowchart simplified material model of Daniel et al[21]

TABLE 1 Material parameters: simplified material model of Daniel et al[21,27]

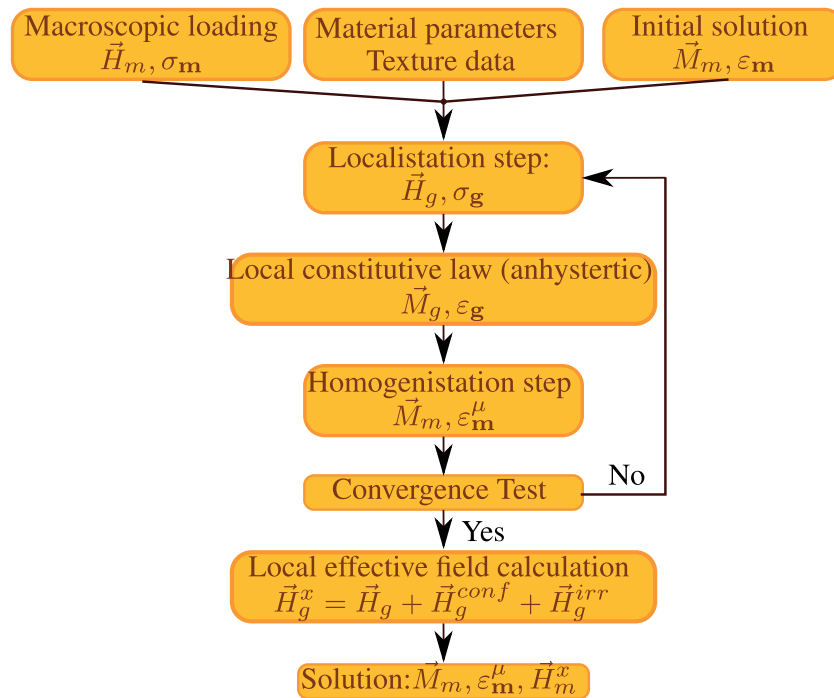| Material	M_s	J	λ_s	A_s	η	k_r^0	c_r	k_a	κ^{ini}
FeSi3%	$1.45 10^6$	0	$12 10^{-6}$	$3.5 10^{-3}$	$2 10^{-4}$	150	0.1	$19 10^{-6}$	1
Unit	A/m	J/m^3	m/m	m^3/J	-	J/m^3	-	m/A	-

FIGURE 2 Flowchart full material model of Daniel et al[6]

for different (uniaxial) stresses, 2 magnetostriction measurements at high fields (perpendicular to each other), and a major hysteresis loop when no stress is applied.[26] Although more material parameters are required, compared to the simplified model, M_s, K_1, K_2, λ_{100}, λ_{111}, C_{11}, C_{12}, and C_{44} are defined at the crystal scale. They are standard physical constants that can be found in physics textbooks like Bozorth[4] and Cullity and Graham,[24] which is an improvement.

5.4 | Our material model

Figure 4 shows the variation of the multiscale energy-based material. The main difference between the full model and our model is the use of the hysteresis energy density function (Equation 6) at the constitutive law, see Sections 2.2 and 3.1. This means the hysteretic distribution P_g (Equation 9) instead of the anhysteretic distribution P_α is used. The self-consistent
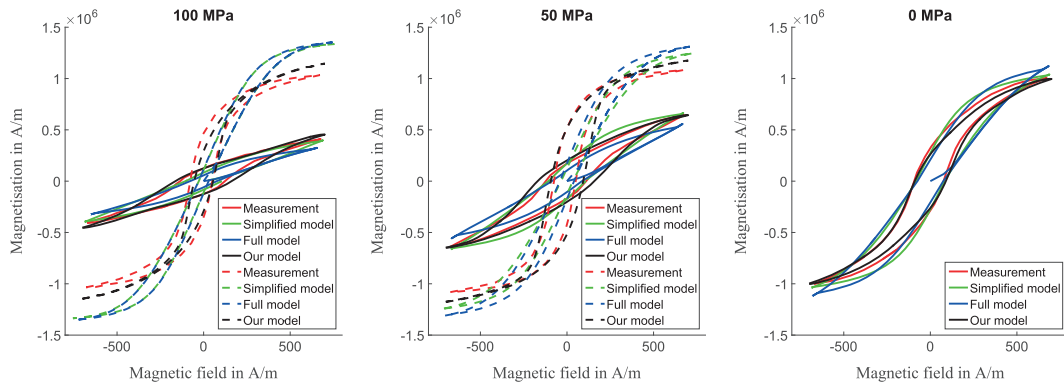
FIGURE 3 Simulated major loops of nonoriented FeSi3% with the different models and the measurements. This is done for different levels of applied mechanical stress, a tensile stress is indicated with a dotted line, whereas compressive stress is indicated with a continuous line

TABLE 2 Material parameter: full material model of Daniel et al[4,6,24,27]

Material	M_s	K_1	K_2	λ_{100}	λ_{111}	C_{11}	C_{12}	C_{44}
FeSi3%	1.6110^6	38	0	2310^{-6}	-4.510^{-6}	20210^9	12210^9	22910^9
Unit	A/m	J/m^3	J/m^3	m/m	m/m	Pa	Pa	Pa
Material	A_s	σ^c	η	k_r^0	c_r	k_a	κ^{ini}	
FeSi3%	310^{-3}	2010^6	210^{-4}	150	0.1	1510^{-6}	1	
Unit	m^3/J	Pa	-	J/m^3	-	m/A	-	
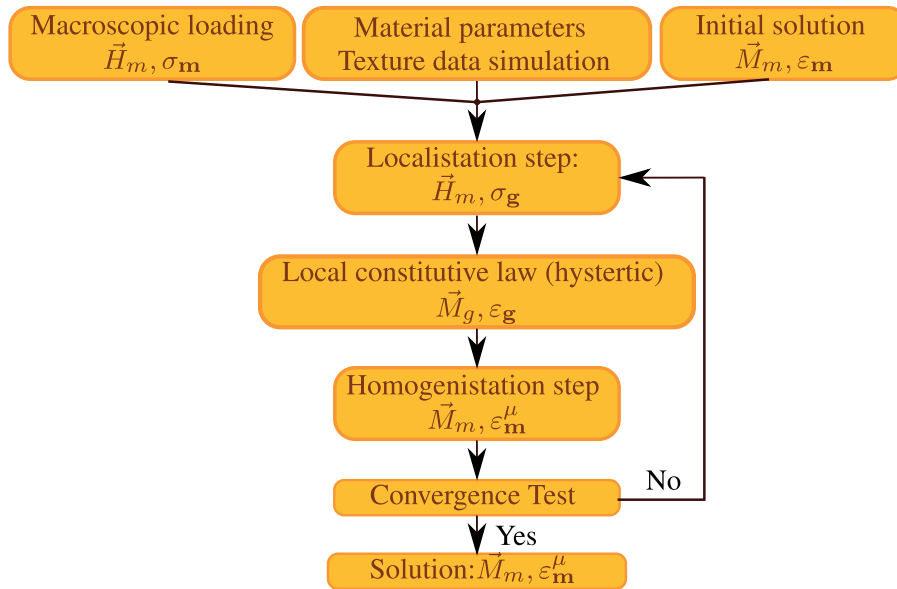
FIGURE 4 Flowchart full material model[17]

TABLE 3 Material Parameters: own model[4,6,17,24,27]

Material	M_s	K_1	K_2	λ_{100}	λ_{111}	C_{11}	C_{12}	C_{44}
FeSi3%	1.6110^6	38	0	2310^{-6}	-4.510^{-6}	20210^9	12210^9	22910^9
Unit	A/m	J/m^3	J/m^3	m/m	m/m	Pa	Pa	Pa

polycrystalline scheme as described in Section 3.2 requires crystallographic texture data that is used with the difference that the crystallographic texture data is simulated instead of measured according to other studies.[17,22,23] The used param-

eters to obtain the simulated results of Figure 3 are given in Table 3. As described in Vanoost,[17] the required material parameters are almost all defined at the crystal scale. This means they are standard physical constants that can be found

in physics textbooks like Bozorth[4] and Cullity and Graham,[24] The parameter A_s is calculated according to Daniel et al and Vanoost et al[16,17] $A_s = \frac{3\chi_0}{\mu_0 M_s^2}$, while the parameter β depends on σ^{eq}. For FeSi3% β equals (Equation 27) with σ^{eq} obtained using Equation 21.

$$\beta = -9 \cdot 10^{-26}(\sigma^{eq})^3 - 3 \cdot 10^{-17}(\sigma^{eq})^2 - 6 \cdot 10^{-10}(\sigma^{eq}) + 0.9372 \tag{27}$$

6 | CONCLUSIONS

This paper compares 3 different energy-based material models, namely, the simplified material model of Daniel et al,[21] the full material model of Daniel et al,[6] as well as our own material model.[17] All these models are able to predict the measured magneto-elastic behavior, but our model predicted this without the need of tedious parameter identification work and is able to take the nonmonotonic effect in consideration. It is shown that by using the hysteresis energy density function, we are able to obtain good agreement between simulation and measurement. Our model uses only standard physical constants which can be found in physics textbooks, with the exception of β. Therefore, further research is required on this parameter β, to obtain a material model that uses only standard physical constants.

REFERENCES

1. Bernard L, Mininger X, Daniel L, Krebs G, Bouillault F, Gabsi M. Effect of stress on switched reluctance motors: a magneto-elastic finite-element approach based on multiscale constitutive laws. *IEEE Trans Magn*. 2011;47(9):2171-2178. https://doi.org/10.1109/TMAG.2011.2145387

2. Ganet F, Hubert O, Mininger X, Bouillault F, Bernard L. Application of the magneto-mechanical coupling to the prediction of deformation of non-oriented FeSi based transformers. In: COMPUMAG 2013, Jun 2013, Budapest, Hungary; 2013.

3. Villari E. Change of magnetization by tension and by electric current. *Ann Phys Chem*. 1865;126:87-122.

4. Bozorth R. *Ferromagnetism (The bell telephone laboratories. The bell telephone laboratories series)*. (9th print. ed.) Princeton (N.J.) Van Nostrand; 1968.

5. Buckley OE, McKeehan LW. Effect of tension upon magnetization and magnetic hysteresis in permalloy. *Phys Rev A*. August 1925;26:261-273. https://doi.org/10.1103/PhysRev.26.261

6. Daniel L, Rekik M, Hubert O. A multiscale model for magneto-elastic behaviour including hysteresis effects. *Arch Appl Mech*. 2014;84(9-11):1307-1323. https://doi.org/10.1007/s00419-014-0863-9

7. LoBue M, Sasso C, Basso V, Fiorillo F, Bertotti G. Power losses and magnetization process in FeSi non-oriented steels under tensile and compressive stress. *J Magn Magn Mater*. 2000;215216:124-126. https://doi.org/10.1016/S0304-8853(00)00092-5. http://www.sciencedirect.com/science/article/pii/S0304885300000925. Accessed June 2, 2000

8. Perevertov O, Schäfer R. Influence of applied tensile stress on the hysteresis curve and magnetic domain structure of grain-oriented Fe–3% Si steel. *J Phys D: Appl Phys*. 2014;47(18):223-228.

9. Sablik MJ, Jiles DC. Coupled magnetoelastic theory of magnetic and magnetostrictive hysteresis. *IEEE Trans Magn*. 1993;29(4):2113-2123.

10. Bergqvist A, Engdahl G. A stress-dependent magnetic Preisach hysteresis model. *IEEE Trans Magn*. November 1991;27(6):4796-4798. https://doi.org/10.1109/20.278950

11. DeSimone A, Kohn RV, Müller S, Otto F. Magnetic microstructures–a paradigm of multiscale problems. In: Ball JM, Hunt JCR, eds. *ICIAM 99*. Oxford: Oxford University Press; 2000:175-190.

12. Néel L. Les lois de l'aimantation et de la subdivision en domaines élémentaires d'un monocristal de fer (in french). *J Phys Radium*. 1944;5(12):265-276.

13. Thoelke J, Jiles D. Model calculation for determining local energy minima in the orientation of magnetic domains in terbium-dysprosium-iron single crystals. *J Magn Magn Mater*. 1992;104-107, Part 2(0):1453-1454. https://doi.org/10.1016/0304-8853(92)90660-G. http://www.sciencedirect.com/science/article/pii/030488539290660G, Proceedings of the International Conference on Magnetism, Part {II}. Accessed February 2 ,1992.

14. Eshelby JD. The determination of the elastic field of an ellipsoidal inclusion and related problems. *Proc Roy Soc A*. 1957;241(1226):376-396.

15. Mura T. *Micromechanics of Defects in Solids*. 2nd, Rev. Ed., Repr. with Minor Corr. ed. Dordrecht: Kluwer Academic; 1991. Print. Mechanics of Elastic and Inelastic Solids.

16. Daniel L, Hubert O, Buiron N, Billardon R. Reversible magneto-elastic behavior: a multiscale approach. *J Mech Phys Solids*. 2008;56(3):1018-1042. https://doi.org/10.1016/j.jmps.2007.06.003. http://www.sciencedirect.com/science/article/pii/S0022509607001263. Accessed March 2008

17. Vanoost D, Steentjes S, Peuteman J, et al. Magnetic hysteresis at the domain scale of a multi-scale material model for magneto-elastic behaviour. *J Magn Magn Mater*. 2016;414:168-179. https://doi.org/10.1016/j.jmmm.2016.04.028. http://www.sciencedirect.com/science/article/pii/S0304885316303420. Accessed September 15, 2016

18. Armstrong WD. The magnetization and magnetostriction of Tb0.3Dy0-7Fe1.9 fiber actuated epoxy matrix composites. *Mater Sci Eng B*. 1997;47(1):47-53. https://doi.org/10.1016/S0921-5107(97)02040-0. http://www.sciencedirect.com/science/article/pii/S0921510797020400. Accessed May 1997.

19. Coey J. *Magnetism and Magnetic Materials*. (4th printing ed.). Cambridge: Cambridge University Press; 2014.

20. DeSimone A, James RD. A constrained theory of magnetoelasticity. *J Mech Phys Solids*. 2002;50(2):283-320. https://doi.org/10.1016/S0022-5096(01)00050-3. http://www.sciencedirect.com/science/article/pii/S0022509601000503. Accessed February 2002

21. Daniel L, Hubert O, Rekik M. A simplified 3-D constitutive law for magnetomechanical behavior. *IEEE T Magn*. 2015;51(3):1-4.

22. Vanoost D, Steentjes S, Peuteman J, et al. Incorporating hysteresis at the grain scale of a multi-scale material model. In: 20th International Conference on the Computation of Electromagnetic Fields (*Compumag*, Montreal, 28 June - 2 July 2015); 2015:PB2-7.

23. Vanoost D, Steentjes S, Peuteman J, et al. Grain scale hysteresis model embedded in a multi-scale material model. In: 2015 IEEE Magnetics Conference International Magnetics Conference (INTERMAG); 11-15 May 2015; Beijin1-1. https://doi.org/10.1109/INTMAG.2015.7156789

24. Cullity BD, Graham CD. *Introduction to magnetic materials*. 2nd ed. Hoboken: Wiley; 2009.

25. Helnwein P. Some remarks on the compressed matrix representation of symmetric second-order and fourth-order tensors.

Comput Method Appl M. 2001;190(22-23):2753-2770. https://doi.org/10.1016/S0045-7825(00)00263-2. http://www.sciencedirect.com/science/article/pii/S0045782500002632. Accessed February 16, 2001

26. Hauser H. Energetic model of ferromagnetic hysteresis: isotropic magnetization. *J Appl Phys*. 2004;96(5):2753-2767.

27. Rekik M. Measurement and modeling of magneto-mechanical dissipative behavior of high yield stress ferromagnetic materials under multiaxial loading: application for high speed generator [doctoral theses]: École normale supérieure de Cachan - ENS Cachan: Cachan; June 2014. https://tel.archives-ouvertes.fr/tel-01022105. Accessed July 25, 2014